

The H-mode Pedestal and Edge Localized Modes in NSTX

R. Maingi^a, E.D. Fredrickson^b, J.E. Menard^b, N. Nishino^c, A.L. Roquemore^b, S.A. Sabbagh^d, K. Tritz^e, and the NSTX Team

^aOak Ridge National Laboratory, Oak Ridge TN, 37831, USA

^bPrinceton Plasma Physics Laboratory, Princeton, NJ 08543, USA

^cHiroshima University, Japan

^dColumbia University, New York, NY USA

^eJohns Hopkins University, Baltimore, MD USA

The research program of the National Spherical Torus Experiment (NSTX) routinely utilizes the H-mode confinement regime to test and extend beta and pulse length limits. As in conventional aspect ratio tokamaks, NSTX observes a variety of edge localized modes (ELMs) in H-mode. Hence a significant part of the research program is dedicated to ELMs studies.

Several different types of ELMs have been observed in NSTX, including Type I ELMs and Type III ELMs from conventional aspect ratio classifications, and also a

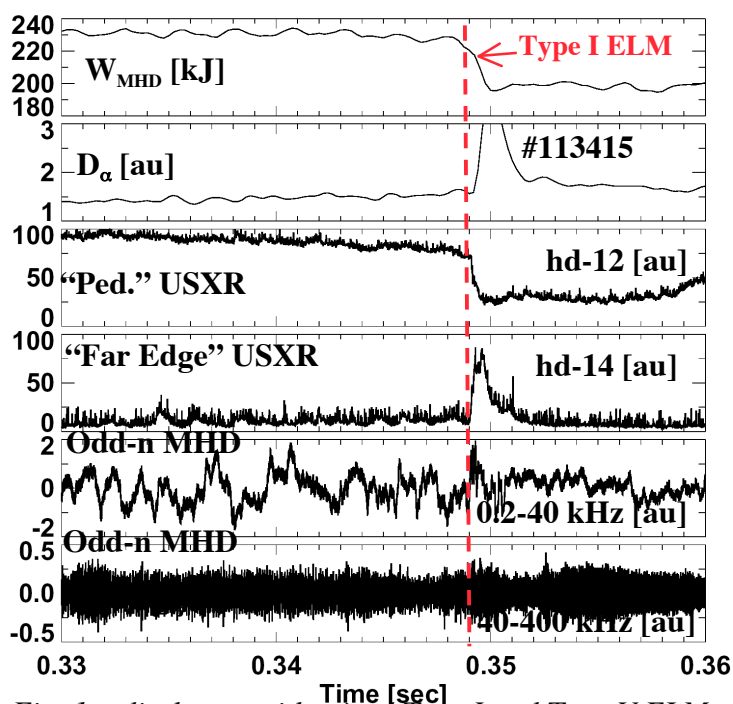


Fig. 1 – discharge with mixed Type I and Type V ELMs. The dashed line indicates time of a Type I ELM. Type V ELMs are observed as the small periodic oscillations prior to the Type I ELM.

new type, which has been labeled[1] as Type V. In NSTX, Type I ELMs are observed with heating power well above the L-H threshold, cause a typical decrease in the stored energy of 5-15%, have no clear electromagnetic precursor, and often result in a cold pulse propagation from the edge into the core. A ‘giant’ version of the Type I ELM has been observed, which can

reduce the stored energy by 30% under certain conditions. Type III ELMs cause a

decrease in the stored energy of <2-3%, have a clear electromagnetic signature and a low frequency pre-cursor < 40 kHz, and are observed in discharges with heating power close to the L-H threshold in certain shapes. Type V ELMs individually cause no measurable decrease in the stored energy, are observed over a wide range of heating power, and have a distinct n=1 mode electromagnetic signature/pre-cursor. These small ELMs can co-exist with Type I ELMs in certain cases.

An example of a mixed Type I/Type V ELM discharge is shown in Fig. 1 ($I_p=0.8$ MA, $B_t=0.45$ T, $P_{\text{NBI}}=6$ MW). Several small type V ELMs are observed on the D_α (panel 1(b)) and ultra-soft X-rays (USXR - panels 1(c) and 1(d)) before the Type I ELM at ~ 0.349 sec. This particular type I ELM decreases the stored energy (W_{MHD})

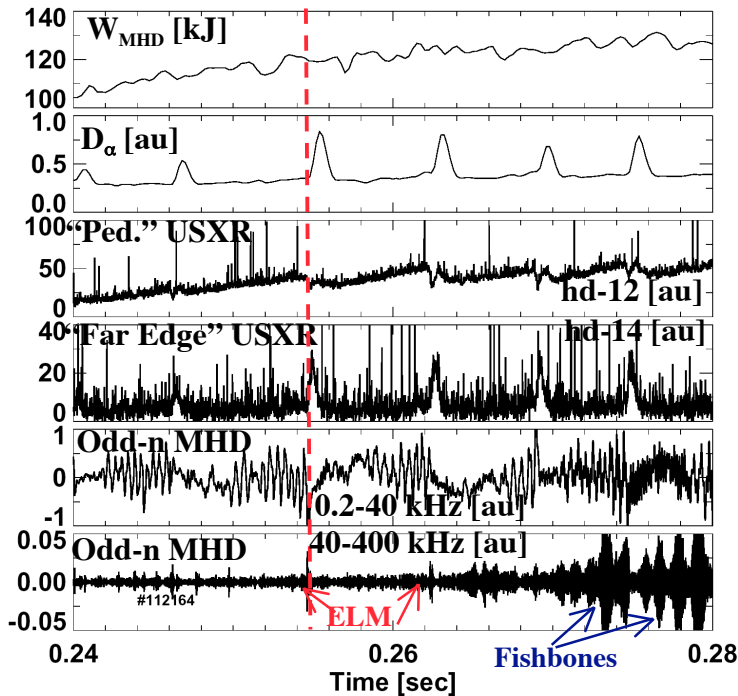


Fig. 2 – discharge with mixed Type III ELMs. The dashed line indicates time of a single Type III ELM, but several others are observed within this time window,

by $\sim 15\%$. As can be seen in panels 1(e) and 1(f), no clear pre-cursor of the Type I ELM is observed in the frequency range from 0.2-400 kHz; the mode itself is apparent in the raw (non-integrated) data with a growth time ~ 150 μsec .

Other Type III ELMs have reduced the stored energy by up to 3%. Panels 2(c) and 2(d) show a drop in the inner USXR data and an increase in the far edge chords, as observed also in the Type I ELM. In contrast to the type I ELM, an inward cold pulse propagation is not observed on the USXR emission. Note also that there is a clear electromagnetic pre-cursor in the 0.2-40 kHz range in panel 2(e), prior to the mode signature in panel 2(f).

An example of a Type III ELM discharge is shown in Fig. 2. It is clear from panel 2(a) that the effect of each of these ELMs is smaller than the statistical error bars of $\pm 1.5\%$. Other Type III ELMs have reduced the stored energy by up to 3%. Panels 2(c) and 2(d) show a drop in the inner USXR data and an increase in the far edge chords, as observed also in the Type I ELM. In contrast to the type I ELM, an inward cold pulse propagation is not observed on the USXR emission. Note also that there is a clear electromagnetic pre-cursor in the 0.2-40 kHz range in panel 2(e), prior to the mode signature in panel 2(f).

As can be seen in panels 1(e) and 1(f), no clear pre-cursor of the Type I ELM is observed in the frequency range from 0.2-400 kHz; the mode itself is apparent in the raw (non-integrated) data with a growth time ~ 150 μsec .

A scaling of the type I ELM energy loss in NSTX was recently reported[2] and is summarized here. The Type I ELM energy loss fraction in that study ($\Delta W_{\text{MHD}}/W_{\text{MHD}}$) was up to 7%, and decreased with increasing line average density. The pedestal stored energy was obtained by fitting the electron pressure profile from Thomson Scattering with a modified hyperbolic tangent function, and using a standard relationship between the pedestal pressure and stored energy. The analysis indicated that the pedestal electron density was typically in the range of $3\text{-}5 \times 10^{19} \text{ m}^{-3}$ and pedestal

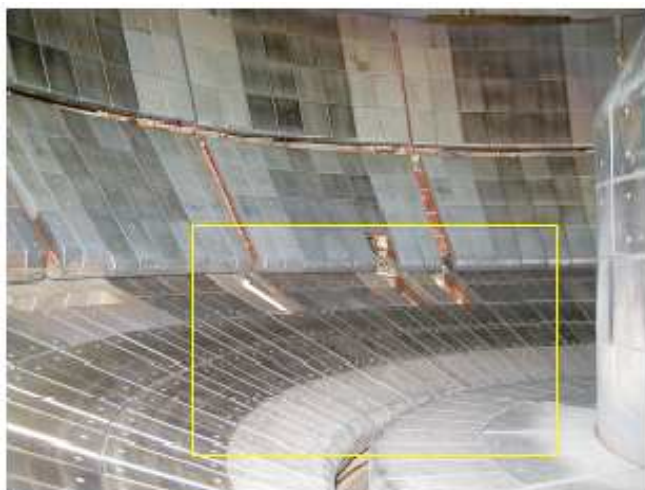


Fig. 3 – tangential view of the NSTX lower divertor region. The image region of the fast framing visible camera is indicated by the yellow box.

electron temperature was in the 200-250 eV range. The pedestal stored energy typically represented between 25-33% of the total stored energy, assuming equal ion and electron temperatures at the top of the pedestal. Thus, the peak pedestal energy loss fractions approached 25-30% for the largest of the Type I ELMs from the study. In certain low recycling regimes in lower-single null configuration,

‘giant’ ELMs were observed which caused a reduction up to 30% of the total stored energy, but these were replaced by Type V ELMs at higher density and fueling rates.

A visible camera capable of up to 40,500 frames per second was installed to view the lower divertor and X-point region during these ELMs. The approximate view of the NSTX divertor with the camera is shown in Fig. 3. The center stack itself is not observed, but for the configurations shown below, the outer strike point and inner separatrix are observed.

The fast camera was used to capture each of the ELM types discussed above. Fig. 4 shows relevant frames from the discharge with Type III ELMs in Fig. 2, and a type I ELM similar to the one in Fig. 3. The inner separatrix is observed as a curve from the lower left to upper right, and the outer strike point is the nearly horizontal arc near the bottom of the image. The top second frame shows the start of the magnetic perturbation, with multiple strike points observed on the outboard side. This splitting

persisted for up to 10 frames ($\sim 250 \mu\text{sec}$), after which a blob of visible light was observed to travel down the inner separatrix (presumably from above) and form a MARFE-like structure along the inner divertor leg, probably in the vicinity of the X-point. The presence of a MARFE is not unexpected because the inner strike point is nearly always detached[3] in NSTX. It is clear that the ELM heat pulse did not burn through this MARFE-like region. Instead the MARFE-like region dissipates approximately 100 frames ($\sim 2.5 \text{ msec}$) before the next Type III ELM, after which the process was repeated for each ELM. We speculate that the long-lived magnetic pre-

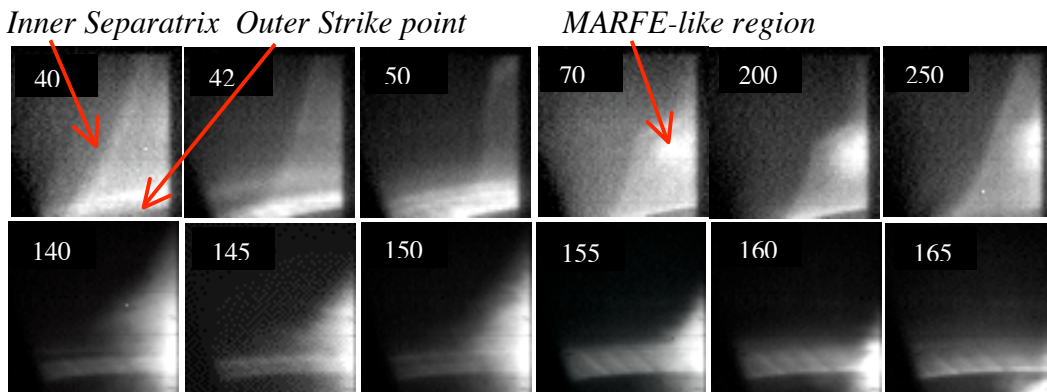


Fig. 4 – unfiltered fast camera images (contrast enhanced) at 40,500 frames per second during one type III ELM for #112164 (upper set) and one Type I ELM for #112503 (lower set). Frame numbers are indicated.

cursor in Panel 2(e) affected the magnetic topology in a way that dissipated the MARFE-like structure. The fast camera images are similar for Type V ELMs, except that the MARFE-like structure did not dissipate between ELMs. However Type I ELMs clearly burned through the MARFE-like region all the way to the target (Fig. 4 – bottom row). The MARFE-like structure was rebuilt on the order of tens of msec. Note that the total light during the Type I ELM was much brighter than the Type III.

In summary, we have presented examples of different ELM types in NSTX. This research was supported by US D.O.E. contracts DE-AC05-00OR22725, DE-AC02-76CH03073, W-7405-ENG-36, and grants DE-FG02-99ER54524, DE-FG02-99ER54519 and DE-FG02-99ER54523.

References

- [1] R. Maingi, et. al., “Observation of a High Performance Mode with Small ELMs in NSTX”, submitted to *Phys. Rev. Letts.*, 5/04.
- [2] R. Maingi, et. al., “ELMs and the H-mode Pedestal in NSTX”, submitted to *J. Nucl. Mater.*, 5/04.
- [3] V.A. Soukhanovskii, et. al., “Analyses of Divertor Regimes in NSTX”, submitted to *J. Nucl. Mater.*, 5/04.